

Osmolytes Induce Structure in an Early Intermediate on the Folding Pathway of Barstar*

Received for publication, June 7, 2004, and in revised form, July 16, 2004
Published, JBC Papers in Press, July 17, 2004, DOI 10.1074/jbc.M406323200

Lovy Pradeep and Jayant B. Udgaonkar‡

From the National Centre for Biological Sciences, Tata Institute of Fundamental Research,
Gandhi Krishi Vigyan Kendra Campus, Bangalore 560 065, India

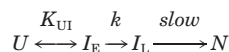
Osmolytes stabilize proteins against denaturation, but little is known about how their stabilizing effect might affect a protein folding pathway. Here, we report the effects of the osmolytes, trimethylamine-*N*-oxide, and sarcosine on the stability of the native state of barstar as well as on the structural heterogeneity of an early intermediate ensemble, I_E , on its folding pathway. Both osmolytes increase the stability of the native protein to a similar extent, with stability increasing linearly with osmolyte concentration. Both osmolytes also increase the stability of I_E but to different extents. Such stabilization leads to an acceleration in the folding rate. Both osmolytes also alter the structure of I_E but do so differentially; the fluorescence and circular dichroism properties of I_E differ in the presence of the different osmolytes. Because these properties also differ from those of the unfolded form in refolding conditions, different burst phase changes in the optical signals are seen for folding in the presence of the different osmolytes. An analysis of the urea dependence of the burst phase changes in fluorescence and circular dichroism demonstrates that the formation of I_E is itself a multi-step process during folding and that the two osmolytes act by stabilizing, differentially, different structural components present in the I_E ensemble. Thus, osmolytes can alter the basic nature of a protein folding pathway by discriminating, through differential stabilization, between different members of an early intermediate ensemble, and in doing so, they thereby appear to channel folding along one route when many routes are available.

Osmolytes are specific amino acids, polyols, and methylamines (1) that are synthesized by microorganisms, plants, and animals in response to environmental stress and that serve to protect proteins against denaturation (1–3). The mechanism by which they stabilize proteins has been studied extensively (1, 4–6). An osmolyte increases the chemical potential of a protein via weak interactions (7). The unfavorable interaction of the osmolyte with the peptide backbone causes the preferential exclusion of the osmolyte from the protein-water interface, and it dominates over any favorable interaction of the osmolyte with the side chains of amino acids of the protein (8, 9). Osmolytes can also induce the folding of proteins, which are

otherwise unfolded. For example, in the presence of the osmolyte TMAO,¹ reduced carboxyamided RNase T₁ and the destabilized T62P mutant of staphylococcal nuclease A, whose unfolded ensembles dominate in native buffers, are forced to fold into forms that are native-like in their secondary and tertiary structural contents (10). TMAO has also been shown to induce structure in α -synuclein, which is unstructured in its absence (11). Thus, osmolytes can not only stabilize folded proteins, but they also appear to be capable of stabilizing the more structured members in an ensemble of disordered protein molecules. It is therefore surprising that very little is known about whether and how osmolytes can affect events on protein folding pathways on which less structured intermediates transform progressively into more structured and stabilized forms. Osmolytes can be expected to perturb not only the transitions between intermediates that differ in stability (12, 13) but also to perturb the equilibria between the differently structured components that may be members of an intermediate ensemble.

Such effects of osmolytes on protein folding pathways have become important to study, because recent studies of the products of the submillisecond folding reactions of several proteins, including barstar (14), ribonuclease A (15, 16), lysozyme (17), cytochrome *c* (18), and apomyoglobin (19), suggest that these early intermediates are structurally heterogeneous. So far, this heterogeneity has manifested itself in two or three co-existing forms (14–21). Because structural heterogeneity is likely to be a consequence of the availability of multiple folding routes, these results suggest that only a few, and not many (22–25), pathways may be available for folding and unfolding, as borne out by experimental studies of the folding and unfolding of several proteins (14, 20, 26–30). It is of great interest to determine whether different protein folding pathways predominate in the presence of different osmolytes, because this will imply that the folding pathways utilized in the cell depend on the conditions present within it.

The 89-amino acid residue, single domain protein barstar is the intracellular inhibitor of the extracellular ribonuclease, barnase in *Bacillus amyloliquefaciens*. The folding mechanism of barstar has been characterized in detail (14, 20, 31–33). Under strongly stabilizing conditions, the folding of barstar can be represented as follows:



SCHEME 1

I_E represents an early intermediate that is populated at a few milliseconds of folding and that equilibrates with U prior to the major structural transition to I_L , a late intermediate.

¹ The abbreviation used is: TMAO, trimethylamine-*N*-oxide.

* This work was funded by the Tata Institute of Fundamental Research and a grant from the Department of Science and Technology of the Government of India. The costs of publication of this article were defrayed in part by the payment of page charges. This article must therefore be hereby marked "advertisement" in accordance with 18 U.S.C. Section 1734 solely to indicate this fact.

‡ Recipient of a Swarnajayanti Fellowship from the Government of India. To whom correspondence should be addressed. Tel.: 91-80-23636420; Fax: 91-80-23636662; E-mail: jayant@ncbs.res.in.

Earlier studies had indicated that I_E is compact and possesses solvent-exposed hydrophobic patches (14). In marginally stabilizing conditions (1–1.2 M guanidine HCl), no specific structure is found to form at a few milliseconds of folding, suggesting either that I_E was devoid of specific structure (33) or that I_E does not accumulate significantly under these folding conditions. There is strong evidence for structural heterogeneity in I_E , from several studies. In the first of these studies, which was the first demonstration of structural heterogeneity in the folding intermediate of any protein, I_E was shown to comprise of at least two structural components that form on competing folding pathways from the same population of U molecules (14). More recent studies indicate that I_E is an ensemble of at least three different structural forms, each of which is stabilized differentially, and hence populated differentially, in the absence and presence of salts (20). I_L also shows structural heterogeneity (34). Most recently, the use of a multi-site time-resolved fluorescence resonance energy transfer approach has shown that the extent of structural heterogeneity depends on how stable the folding conditions are and that different structural components predominate in I_L under different folding conditions (35). Obviously, barstar is a good model system for exploring the effects of osmolytes on the structural heterogeneity that now appears characteristic of protein folding reactions.

In this study, fluorescence and circular dichroism have been used to study the effects of osmolytes on the stability of the native state and on the heterogeneity of the protein folding reactions. It is seen that the free energy of unfolding of the N state of barstar to the U form has a linear dependence on TMAO as well as on sarcosine concentration, suggesting that the mechanism of stabilization by both osmolytes primarily involves their preferential exclusion from the protein surface. Next, it is shown that the structure of the early intermediate ensemble, I_E , is altered, significantly and differentially, in the presence of 1 M TMAO and sarcosine. The heterogeneity in I_E has been characterized, and it is shown that the two osmolytes, TMAO and sarcosine, differentially stabilize structure in I_E by shifting the equilibrium between different structural components to favor the more structured components. Finally the use of osmolytes has led to a better understanding of the folding pathway of barstar; the transition from the unfolded protein in refolding conditions to I_E , is shown to occur through more than one step in the presence of the osmolytes.

EXPERIMENTAL PROCEDURES

Bacterial Strain and Plasmid and Protein Purification

The *Escherichia coli* strain MM294 was used for protein expression. The expression plasmid for wild-type barstar was pMT316. The method used to purify barstar has been described in detail (36). Protein concentrations were calculated using an extinction coefficient of $23,000 \text{ M}^{-1} \text{ cm}^{-1}$ (36). Mass spectroscopy using a Micromass Q-TOF Ultima showed that the protein was pure and had a mass of 10342, which indicated that the N-terminal methionine residue had remained uncleaved during synthesis.

Buffers and Solutions

30 mM Tris-HCl (pH 8) (ultrapure, 99.9% from Invitrogen), 250 μM EDTA (disodium salt, dihydrate, 99+% from Sigma), and 250 μM dithiothreitol (ultrapure from Invitrogen) constituted the native buffer used for all equilibrium and kinetic experiments. Unfolding buffer was native buffer containing 9 to 10 M urea (ultrapure, 99.9% from United States Biochemical). The concentrations of stock solutions of urea were determined by measuring the refractive index using an Abbe 3L refractometer from Milton Roy. For folding studies in the presence of osmolyte (TMAO or sarcosine), the osmolyte was present in the refolding as well as in the unfolding buffer. The unfolding buffers containing 1 M TMAO (dihydrate, ultrapure from Sigma) or 1 M sarcosine (ultrapure from Sigma) had a maximum urea concentration of 9 M, because of solubility

limitations. All of the buffers and solutions were filtered through 0.22- μm filters before use and were degassed prior to the kinetic experiments.

Spectroscopic Characterization

CD spectra were collected on a Jasco J720 spectropolarimeter, using a bandwidth of 1 nm, a response time of 1 s, and a scan speed of 50 nm/min. Each spectrum was an average of three scans monitored between 210 and 250 nm. The protein concentration used was typically 10–15 μM for the far-UV CD experiments, and the path length of the cuvette was 0.2 cm. Fluorescence spectra were collected on a SPEX DM 3000 spectrofluorimeter. The protein was excited at 295 nm, and the emission was monitored between 300 and 400 nm with a bandwidth of 0.37 nm for excitation and 10 nm for emission. Each spectrum was an average of three scans. The protein concentration was typically 2–4 μM , and the path length of the cuvette used was 1 cm.

Equilibrium Unfolding Studies

Protein stability at equilibrium was determined by urea-induced denaturation studies using two probes. The CD at 222 nm and fluorescence at 320 nm were monitored as described above. Prior to the CD and fluorescence measurements, the samples were equilibrated for at least 4 h. Identical results were obtained if the time of incubation was 24 h.

Kinetic Experiments

Kinetic experiments were performed on a Biologic SFM-4 stopped-flow mixing module. Folding was monitored using either intrinsic tryptophan fluorescence at 320 nm or far-UV CD at 222 nm as the probe.

Intrinsic Tryptophan Fluorescence Measurements—For intrinsic tryptophan fluorescence measurements, the excitation wavelength was set at 295 nm, and emission was monitored at 320 nm using an Oriel bandpass filter with a bandwidth of 10 nm. The protein concentration during refolding was between 15 and 30 μM . In all experiments, an FC-08 cuvette with a path length of 0.8 mm was used, the total flow rate was 6.0 ml/s, and the dead time of the instrument was 1.5 ms. For refolding experiments, barstar was unfolded in 9 M urea (unfolding buffer) for at least 4 h (the unfolding buffer contained TMAO or sarcosine when refolding was studied in the presence of osmolyte). In refolding experiments, the final concentration of urea was between 0.9 and 2.7 M in the absence of osmolyte and between 0.9 and 4.5 M in the presence of 1 M TMAO or 1 M sarcosine.

Far-UV CD Measurements—For far-UV CD measurements, a polarizer/modulator assembly was installed on the Biologic SFM-4 stopped-flow mixing module. A photomultiplier and its controller (model PMS 400) was used to collect data in the CD mode. A test experiment was performed to check the performance of the CD recording system for proper alignment of the optics and the polarizer/modulator assembly, in which the alkaline hydrolysis of glucuronolactone at 225 nm was studied. For all of the kinetic studies on the folding of barstar, the wavelength was set to 222 nm, and the retardation was set to $\frac{1}{4}$ wavelength. The protein concentration during refolding was between 15 and 25 μM ; the upper limit was decided based on a pilot experiment, wherein linearity in the CD signal was found to be lost at concentrations above 25 μM . In all experiments, an FC-20 cuvette with a path length of 2.0 mm was used, the total flow rate was 6.0 ml/s, and the dead time was 9.0 ms. For refolding experiments, barstar was unfolded in 9 M urea (unfolding buffer) for at least 4 h (the unfolding buffer contained TMAO or sarcosine when refolding was studied in the presence of osmolyte). In refolding experiments, the final concentration of urea was between 0.9 and 2.7 M in the absence of osmolyte and between 0.9 and 4.5 M in the presence of 1 M TMAO or 1 M sarcosine. The kinetics on this module could be collected only for 20 s because of bleaching. Far-UV CD kinetics for longer time periods were collected manually on a Jasco J720 spectropolarimeter, using a bandwidth of 1 nm, a response time of 1 s, and a sensitivity of 50 millidegrees. Each kinetic trace was an average of three kinetic runs at 222 nm. The protein concentration used was typically 15–25 μM for the far-UV CD experiments, the path length of the cuvette was 2.0 mm, and the dead time for manual kinetics was 20 s.

Data Analysis

Equilibrium Studies—According to the weak interaction (linear free energy) model for describing the interaction of urea (D) with a protein (7, 37), the change in free energy, ΔG , that occurs upon unfolding of any form of a protein, j , in the presence of D, is linearly dependent on denaturant concentration, [D].

$$\Delta G'_{Uj} = \Delta G_{Uj} + m_{Uj}[D] \quad (\text{Eq. 1})$$

m_{Uj} is the change in free energy associated with the preferential interaction of the denaturant with the unfolded form, U , relative to the folded (partially or fully) form, j . When the form j is a partially folded intermediate I , $\Delta G'_{UI}$, represents the free energy of unfolding of I , and when j is the native state, N , $\Delta G'_{UN}$ represents the free energy of unfolding of N in the presence of denaturant. ΔG_{Uj} represents the free energy of unfolding of the folded (partially or fully) form j to U in the absence of any denaturant or added co-solute.

An osmolyte, O , acting as a chemical perturbant, also interacts with a protein according to the weak interaction model (38), and the free energy of unfolding of a folded form j to U , in the presence of O , has a linear dependence on osmolyte concentration, $[O]$.

$$\Delta G''_{Uj} = \Delta G_{Uj} + m''_O[O] \quad (\text{Eq. 2})$$

m''_O is the change in free energy associated with the preferential interaction of the osmolyte with the unfolded form, U , relative to the folded (partially or fully) form, j . According to Equation 2, m''_O has a positive value when the folded form is stabilized in the presence of osmolyte. When the form j is a partially folded intermediate I , $\Delta G''_{UI}$, represents the free energy of stabilization of I , and when j is the native state, N , $\Delta G''_{UN}$ represents the free energy of stabilization of N , in the presence of osmolyte.

Thus, in the presence of both denaturant and osmolyte, the free energy of unfolding of a folded form, j to the unfolded form U , $\Delta G'''_{Uj}$ is given by the following.

$$\Delta G'''_{Uj} = \Delta G_{Uj} + m''_O[O] + m_{Uj}[D] \quad (\text{Eq. 3})$$

Equation 3 assumes that m_{Uj} is independent of $[O]$ and that m''_O is independent of $[D]$.

The equilibrium data for the unfolding of N as a function of $[D]$, obtained in the presence of a fixed concentration of osmolyte, were fit to a two-state $U \rightleftharpoons N$ model according to the following equation,

$$Y_O = \frac{Y_N + m_N[D] + (Y_U + m_U[D]) e^{-\frac{(\Delta G'_{UN} + m_{UN}[D])}{RT}}}{1 + e^{-\frac{(\Delta G'_{UN} + m_{UN}[D])}{RT}}} \quad (\text{Eq. 4})$$

where Y_O is the value of the spectroscopic property being measured as a function of $[D]$ at fixed $[O]$, Y_N and Y_U represents the intercepts, and m_N and m_U represent the slopes of the native protein and unfolded protein base lines, respectively. Thus, fits of denaturant-induced equilibrium unfolding data at different fixed values of $[O]$ to Equation 4 yield values for $\Delta G'_{UN}$ and m_{UN} at each fixed $[O]$, and a subsequent fit of the osmolyte dependence of $\Delta G'_{UN}$ to Equation 2 yields values for $\Delta G''_{UN}$ and m''_O .

Raw equilibrium unfolding data of N as a function of $[D]$ were also analyzed in an alternative way (39). They were first converted to plots of fraction unfolded (f_U) versus $[D]$, using Equation 5.

$$f_U = \frac{Y_O - (Y_N + m_N[D])}{(Y_U + m_U[D]) - (Y_N + m_N[D])} \quad (\text{Eq. 5})$$

The f_U values were then fit to Equation 6.

$$f_U = \frac{e^{-\frac{(\Delta G'_{UN} + m_{UN}[D])}{RT}}}{1 + e^{-\frac{(\Delta G'_{UN} + m_{UN}[D])}{RT}}} \quad (\text{Eq. 6})$$

In Equation 6, f_U is related to $\Delta G'_{UN}$ by a transformation of the Gibbs-Helmholtz equation in which the equilibrium constant for unfolding in the transition zone, K'_{UN} , is given by $K'_{UN} = f_U/(1 - f_U)$, for a two-state transition.

The concentration of the denaturant at which the protein is half unfolded (when $\Delta G'_{Uj} = 0$), is given by C_m and from Equation 1, $C_m = \Delta G_{Uj}/m_{Uj}$.

Kinetic Studies—The observable kinetics of folding of barstar in the pretransition zone are described by a three-exponential process when monitored by fluorescence at 320 nm:

$$A(t) = A(\infty) - A_1 e^{-\lambda_1 t} - A_2 e^{-\lambda_2 t} - A_3 e^{-\lambda_3 t} \quad (\text{Eq. 7})$$

where $A(t)$ and $A(\infty)$ are the observed reduced amplitudes at times t and at infinity; λ_1 , λ_2 and λ_3 are the apparent rate constants of the slow, fast and intermediate phases, and A_1 , A_2 and A_3 are the respective amplitudes. The relative amplitude of each phase was determined by dividing

the observed amplitude of that phase by the equilibrium amplitude of the reaction at that urea concentration. In the transition zone, the folding process is two-exponential and is described by Equation 7, with $A_3 = 0$.

The observable kinetics of folding of barstar in the pretransition zone and transition zone are described by a two-exponential process when monitored by CD at 222 nm,

$$A(t) = A(\infty) - A_1 e^{-\lambda_1 t} - A_2 e^{-\lambda_2 t} \quad (\text{Eq. 8})$$

or by a single exponential process, by setting A_1 equal to zero in Equation 8, at lower urea concentrations in the pretransition zone. In the absence of any osmolyte, for refolding at the lowest urea concentration, *i.e.* 0.9 M urea, no slow phase was observed; the signal corresponding to that of the N state was achieved in the dead time (20 s) of a manual mixing experiment, and no slow phase is observable in a stopped-flow experiment. For slightly higher urea concentrations (1.5 and 1.8 M), the $t = \infty$ of the stopped-flow kinetic data coincides with the $t = 0$ of the manual mixing kinetic data. But for the urea concentrations 2.1, 2.4, and 2.7 M, the $t = \infty$ of the stopped-flow kinetic data did not coincide with the $t = 0$ of the manual mixing kinetic data. That is, at higher concentrations of urea, there was a 5–14% discrepancy between the equilibrium folding amplitude and amplitude of the observable kinetic phases and the burst phase. Likewise, in the presence of either osmolyte, only the fast phase of refolding was observed at urea concentrations below 2.7 M. At higher urea concentrations, the $t = \infty$ from the stopped-flow measurements again did not coincide with the $t = 0$ of the manual mixing experiments, with there being a maximum discrepancy of up to 10% in amplitudes. The discrepancy was possibly due to the contribution of linear dichroism (arising from pressure on the cuvette) to the observed protein signal, which probably is also responsible for the 2–3-millidegree discrepancy observed between the signal of unfolded protein (9 M urea) measured on the Jasco J720 spectropolarimeter and on the Biologic SFM 4. Thus, there is about a 10–15% error in the data of the amplitudes at the higher concentrations of urea used.

To analyze kinetic data according to Scheme 1, it was assumed that the conformational transitions between U , U_C , and I_E are rapid compared with the subsequent slow conversion of I_E to I_L and N , so that a transient pre-equilibrium, characterized by the equilibrium constant, K_{UI} , is established between U_C and I_E .

To determine whether the transition between two U_C and I_E is two-state, the pre-equilibrium data for the denaturant-induced unfolding of I_E , obtained from kinetic experiments in the presence of a fixed concentration of osmolyte, O , as well as the pre-equilibrium data for the osmolyte-induced stabilization of I_E at a fixed concentration of denaturant, were fit to a two-state model according to the following equation,

$$Y = \frac{Y_I + m_I[X] + (Y_U + m_U[X]) e^{-\frac{(\Delta G_{UI} + m_{UI}[D] + m'_I[O])}{RT}}}{1 + e^{-\frac{(\Delta G_{UI} + m_{UI}[D] + m'_I[O])}{RT}}} \quad (\text{Eq. 9})$$

where $[X]$ is the variable $[D]$ for experiments in which refolding is carried out at a fixed value of $[O]$, and $[X]$ is the variable $[O]$ for experiments in which refolding is carried out at a fixed $[D]$. Y is the value of the spectroscopic property being measured as a function of the variable $[X]$, Y_I and Y_U represent the intercepts, and m_I and m_U represent the slopes of the I_E and U_C base lines, respectively.

The dependence of the rate constant, k , for the conversion of I_E to I_L or N (Scheme 1) is expected to decrease exponentially with an increase in $[D]$, because the free energy of activation is expected to increase linearly with an increase in $[D]$. Also, k is expected to increase exponentially with an increase in $[O]$, because the free energy of activation is assumed to decrease linearly with an increase in $[O]$. This is given by the following equation,

$$k = k^0 e^{-m_k^0[D]} e^{m_k^0[O]} \quad (\text{Eq. 10})$$

where k^0 is the rate constant in the absence of denaturant and osmolyte, RTm_k^0 is the free energy associated with the preferential interaction of denaturant with the transition state relative to I_E , and RTm_k^0 is the free energy associated with the preferential interaction of osmolyte with the transition state relative to I_E .

Then the observed rate of folding, λ'' , in the presence of both urea at concentration $[D]$ and osmolyte at concentration $[O]$, is given by the following.

$$\lambda'' = \frac{k}{1 + e^{-\frac{\Delta G'_{UI}}{RT}}} = \frac{k^0 e^{-m_k^0[D]} e^{m_k^0[O]}}{1 + e^{-\frac{(\Delta G_{UI} + m_{UI}[D] + m'_I[O])}{RT}}} \quad (\text{Eq. 11})$$

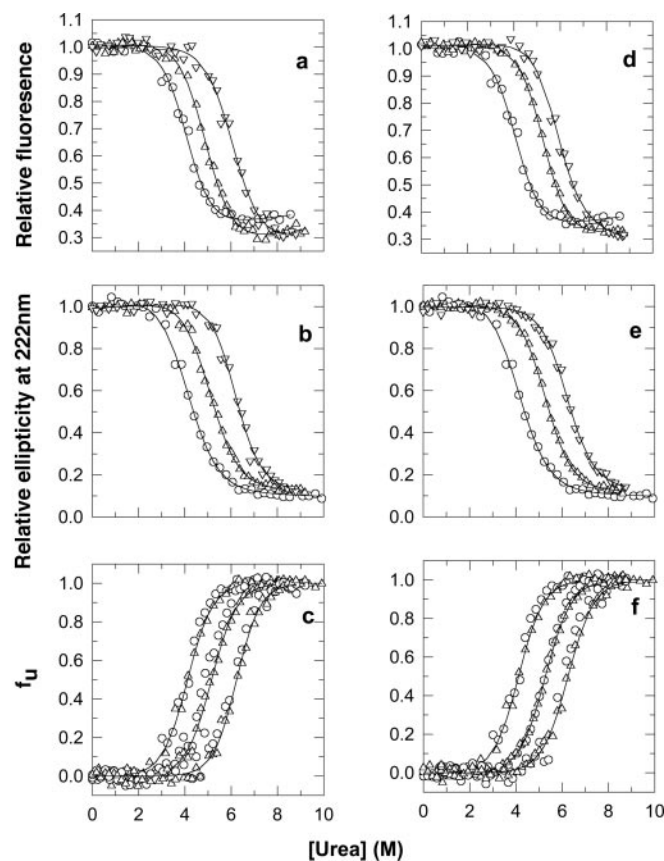


FIG. 1. Stabilization of wild-type barstar by TMAO and sarcosine at pH 8, 25 °C. *a*, equilibrium urea-induced transitions were determined using fluorescence at 320 nm to monitor unfolding in 0 M (○), 0.5 M (△), and 1.0 M (▽) TMAO. The unfolding transitions were fit to Equation 4, and the fits, represented by the *continuous lines*, yielded values for $\Delta G_{\text{UN}}^{\text{H}}$ and m_{UN} of 4.7 kcal mol⁻¹ and -1.15 kcal mol⁻¹ M⁻¹, respectively, in the absence of TMAO; 6.0 kcal mol⁻¹ and -1.2 kcal mol⁻¹ M⁻¹, respectively, in 0.5 M TMAO; and 7.1 kcal mol⁻¹ and -1.16 kcal mol⁻¹ M⁻¹, respectively, in 1.0 M TMAO. *b*, equilibrium urea-induced unfolding transitions were determined using far-UV CD at 222 nm to monitor unfolding in 0 M (○), 0.5 M (△), and 1.0 M (▽) TMAO. The unfolding transitions were fit to Equation 4, and the fits, represented by the *continuous lines*, yielded values for $\Delta G_{\text{UN}}^{\text{H}}$ and m_{UN} of 4.9 kcal mol⁻¹ and -1.17 kcal mol⁻¹ M⁻¹, respectively, in the absence of TMAO; 6.1 kcal mol⁻¹ and -1.17 kcal mol⁻¹ M⁻¹, respectively, in 0.5 M TMAO; and 7.1 kcal mol⁻¹ and -1.14 kcal mol⁻¹ M⁻¹, respectively, in 1.0 M TMAO. *c*, the raw data in *a* and *b* were converted to plots of f_{U} versus urea concentration using Equation 5 and the data fit to Equation 6. The fits are represented by the *continuous lines* through the data. ○, fluorescence; △, far-UV CD. *d*, equilibrium urea-induced transitions were determined using fluorescence to monitor unfolding in 0 M (○), 0.5 M (△), and 1.0 M (▽) sarcosine. The unfolding transitions were fit to Equation 4, and the fits, represented by the *continuous lines*, yielded values for $\Delta G_{\text{UN}}^{\text{H}}$ and m_{UN} of 4.7 kcal mol⁻¹ and -1.15 kcal mol⁻¹ M⁻¹, respectively, in the absence of sarcosine; 6.0 kcal mol⁻¹ and -1.15 kcal mol⁻¹ M⁻¹, respectively, in 0.5 M sarcosine; and 6.9 kcal mol⁻¹ and -1.14 kcal mol⁻¹ M⁻¹, respectively, in 1.0 M sarcosine. *e*, equilibrium urea-induced unfolding transitions were determined using far-UV CD to monitor unfolding in 0 M (○), 0.5 M (△), and 1.0 M (▽) sarcosine. The unfolding transitions were fit to Equation 4, and the fits, represented by the *continuous lines*, yielded values for $\Delta G_{\text{UN}}^{\text{H}}$ and m_{UN} of 4.9 kcal mol⁻¹ and -1.17 kcal mol⁻¹ M⁻¹, respectively, in the absence of sarcosine; 5.9 kcal mol⁻¹ and -1.11 kcal mol⁻¹ M⁻¹, respectively, in 0.5 M sarcosine; and 7.1 kcal mol⁻¹ and -1.13 kcal mol⁻¹ M⁻¹, respectively, in 1.0 M sarcosine. *f*, the raw data in *d* and *e* were converted to plots of f_{U} versus urea concentration using Equation 5 and the data fit to Equation 6. The fits are represented by the *continuous lines* through the data. ○, fluorescence; △, far-UV CD.

RESULTS

Equilibrium Urea-induced Unfolding Transitions in the Absence and in the Presence of 1 M TMAO and 1 M Sarcosine—Fig. 1*a* compares urea-induced equilibrium unfolding transitions of

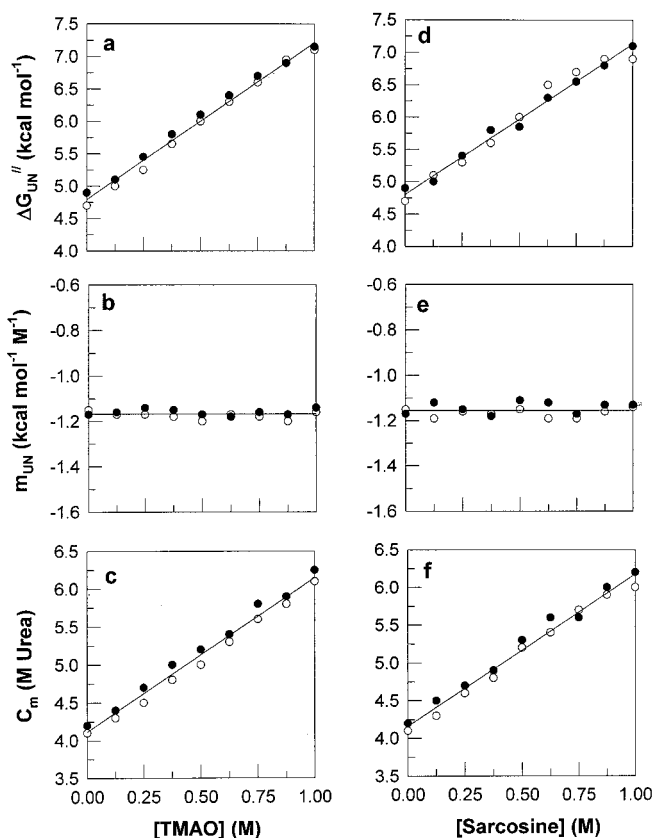


FIG. 2. Effect of TMAO and sarcosine on the thermodynamics of unfolding. Values for $\Delta G_{\text{UN}}^{\text{H}}$ (*a*), m_{UN} (*b*), and C_{m} (*c*) were determined from urea-induced unfolding transitions of barstar in TMAO at pH 8, 25 °C, monitored by fluorescence (○) at 320 nm upon excitation at 295 nm and far-UV CD at 222 nm (●). Values for $\Delta G_{\text{UN}}^{\text{H}}$ (*d*), m_{UN} (*e*), and C_{m} (*f*) were determined from urea-induced unfolding transitions of barstar in sarcosine at pH 8, 25 °C, monitored by fluorescence (○) and far-UV CD (●). The *continuous line* through the data in *a* is a fit of the data to Equation 2 and yields values for $\Delta G_{\text{UN}}^{\text{H}}$ and m_{UN}^{N} of 4.8 kcal mol⁻¹ and 2.42 kcal mol⁻¹ M⁻¹, respectively. The *continuous line* through the data in *b* represents the mean value of m_{UN} (-1.17 kcal mol⁻¹ M⁻¹) averaged over all TMAO concentrations for the fluorescence and CD data. The *continuous line* through the data in *c* is described by, $C_{\text{m(TMAO)}} = 4.11 + 2.03 [\text{TMAO}]$. The *continuous line* through the data in *d* is a fit of the data to Equation 2 and yields values for $\Delta G_{\text{UN}}^{\text{H}}$ and m_{UN}^{N} of 4.8 kcal mol⁻¹ and 2.33 kcal mol⁻¹ M⁻¹, respectively. The *continuous line* through the data in *e* represents the mean value of m_{UN} (-1.15 kcal mol⁻¹ M⁻¹) averaged over all sarcosine concentrations for the fluorescence and CD data. The *continuous line* through the data in *f* is described by $C_{\text{m(sarcosine)}} = 4.16 + 2.01 [\text{sarcosine}]$.

barstar in the absence and presence of TMAO, obtained using tryptophan fluorescence emission at 320 nm as a probe for structure. Fig. 1*d* likewise compares urea-induced equilibrium unfolding transitions in the absence and presence of sarcosine. For both osmolytes, the mid-point of the unfolding transition, C_{m} , increases in value with increasing osmolyte concentration. The data were fit to Equation 4. The values obtained for the free energy of unfolding, $\Delta G_{\text{UN}}^{\text{H}}$, and for the preferential free energy of interaction of urea with the unfolded state relative to with the folded state, m_{UN} , in the absence of any osmolyte are similar to values reported earlier (20, 32). Similar results were obtained when unfolding in TMAO and sarcosine was monitored using far-UV CD at 222 nm (Fig. 1, *b* and *e*, respectively). The data in Fig. 1 (*a*, *b*, *d* and *e*) were converted to plots of fraction of protein unfolded, f_{U} , versus urea concentration, using Equation 5, in Fig. 1 (*c* and *f*), for unfolding transitions in TMAO and sarcosine, respectively. At any concentration of osmolyte, both probes yield overlapping f_{U} plots, indicating

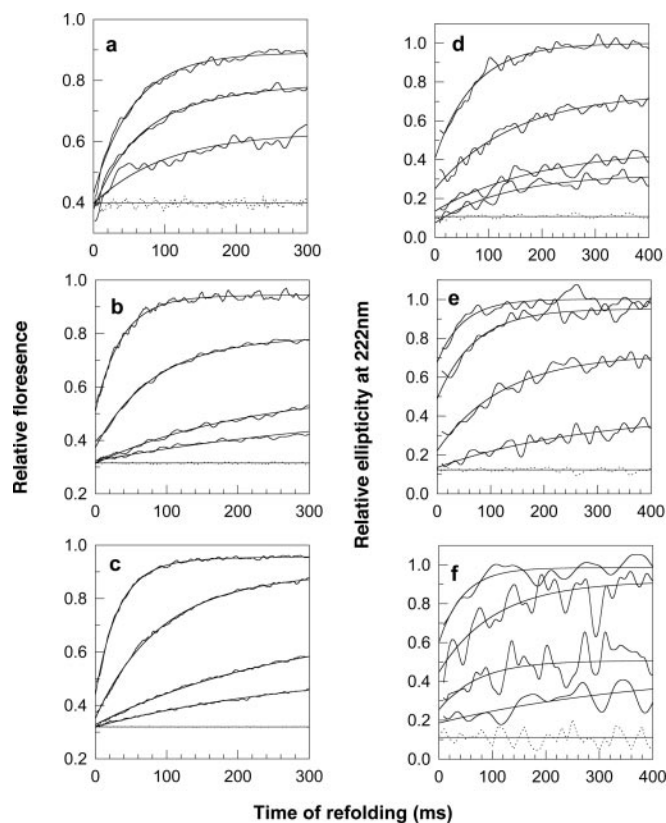


FIG. 3. Kinetics of refolding of barstar in 0 and 1 M TMAO and 1 M sarcosine. *a*, kinetic traces of refolding in 0 M osmolyte. From *top* to *bottom*, representative normalized traces of refolding in three different concentrations of urea, 0.98, 1.63, and 2.28 M, for the first 300 ms, monitored by fluorescence at 320 nm. *b*, kinetic traces of refolding in 1 M TMAO. From *top* to *bottom*, representative normalized traces of refolding in four different concentrations of urea, 0.9, 2.4, 3.9, and 4.5 M, for the first 300 ms, monitored by fluorescence. *c*, kinetic traces of refolding in 1 M sarcosine. From *top* to *bottom*, representative normalized traces of refolding in four different concentrations of urea, 0.9, 2.4, 3.9, and 4.5 M, for the first 300 ms, monitored by fluorescence. *d*, kinetic traces of refolding in 0 M osmolyte. From *top* to *bottom*, representative normalized traces of refolding in four different concentrations of urea, 0.9, 1.8, 2.4, and 2.7 M, for the first 400 ms, monitored by far-UV CD at 222 nm. *e*, kinetic traces of refolding in 1 M TMAO. From *top* to *bottom*, representative normalized traces of refolding in four different concentrations of urea, 0.9, 2.4, 3.9, and 4.5 M, for the first 400 ms, monitored by far-UV CD. *f*, kinetic traces of refolding in 1 M sarcosine. From *top* to *bottom*, representative normalized traces of refolding in four different concentrations of urea, 0.9, 2.4, 3.9, and 4.5 M, for the first 400 ms, monitored by far-UV CD. In each panel, the fluorescence and CD values have been normalized to a value of 1 for fully folded protein; the *dotted line* indicates the signal of unfolded protein at the same protein concentration. The *continuous line* through the unfolded protein signal in each panel is a linear fit with a slope of zero. The *continuous lines* through the data in *a–c* are fits to Equation 7, and the *continuous lines* through the data in *d–f* are fits to Equation 8. The fluorescence data in *a* has been borrowed from Fig. 5 in Ref. 20.

simultaneous loss of tertiary and secondary structure and supporting the assumption made in Equations 4 and 6 that the $U \rightleftharpoons N$ transition is two-state.

It should be noted that the optical spectroscopic properties of barstar are not altered in the presence of TMAO or sarcosine. Fluorescence and CD spectra in the absence and presence of TMAO or sarcosine show that there is no shift in the emission maximum (λ_{\max}) or change in CD for both the N and U forms (data not shown). The N state shows the same intrinsic tryptophan fluorescence intensity in the presence of 1 M TMAO or 1 M sarcosine, whereas the U form shows only a 5% lesser fluorescence intensity in the presence of 1 M TMAO and 1 M sarcosine.

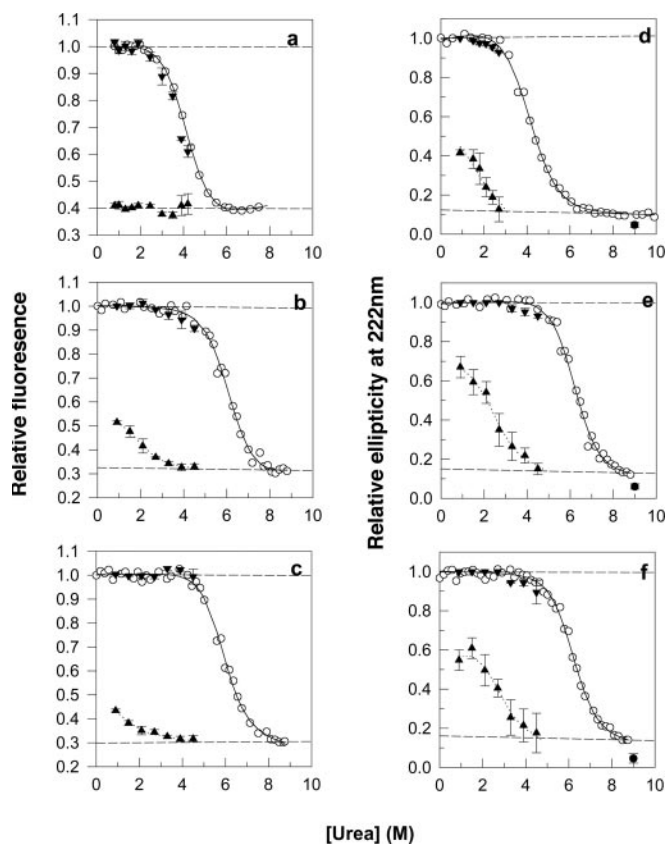


FIG. 4. Kinetic versus equilibrium amplitudes of fluorescence- and CD-monitored folding at pH 8, 25 °C. Kinetic and equilibrium amplitudes of folding in 0 M osmolyte (*a*), 1 M TMAO (*b*), and 1 M sarcosine (*c*) monitored by fluorescence at 320 nm are shown. Kinetic and equilibrium amplitudes of folding in 0 M osmolyte (*d*), 1 M TMAO (*e*), and 1 M sarcosine (*f*), monitored by CD at 222 nm, are also shown. Urea-induced equilibrium unfolding curve (\circ); $t = 0$ points of kinetic folding traces (\blacktriangle); $t = \infty$ points of kinetic folding traces (\blacktriangledown). The *continuous lines* represent nonlinear least square fits of the equilibrium unfolding data to Equation 5. The *dashed lines* represent linearly extrapolated folded and unfolded protein base lines. The *error bars* on the kinetic data points reflect the standard deviations determined from three repetitions of each experiment. The *dotted lines* through the $t = 0$ points of refolding in *b–f* are described by Equation 9. The fit through the $t = 0$ points of refolding in the absence of osmolytes monitored by CD (*d*) yielded values for ΔG_{UI} and m_{UI} of 0.5 kcal mol $^{-1}$ and -0.9 kcal mol $^{-1}$ M $^{-1}$, respectively. The fit through the $t = 0$ points for refolding in 1 M TMAO yielded values for ΔG_{UI} , m_{UI} , and $m_{\text{O}}^{\text{f}}(\text{TMAO})$ of 0.5 kcal mol $^{-1}$, -1.0 kcal mol $^{-1}$ M $^{-1}$, and 0.85 kcal mol $^{-1}$ M $^{-1}$, respectively, when monitored by fluorescence (*b*), and of 0.54 kcal mol $^{-1}$, -1.0 kcal mol $^{-1}$ M $^{-1}$, and 1.9 kcal mol $^{-1}$ M $^{-1}$, respectively, when monitored by CD (*e*). The fit through the $t = 0$ points for refolding in 1 M sarcosine yielded values for ΔG_{UI} , m_{UI} , and $m_{\text{O}}^{\text{f}}(\text{sarcosine})$ of 0.5 kcal mol $^{-1}$, -1.0 kcal mol $^{-1}$ M $^{-1}$, and 1.15 kcal mol $^{-1}$ M $^{-1}$, respectively, when monitored by fluorescence (*c*), and of 0.5 kcal mol $^{-1}$, -1.0 kcal mol $^{-1}$ M $^{-1}$, and 2.1 kcal mol $^{-1}$ M $^{-1}$, respectively, when monitored by CD (*f*). represents the signal of the unfolded protein (9.0 M urea) obtained from stopped-flow CD measurements in *d–f*. The fluorescence data in *a* have been borrowed from Fig. 6 in Ref. 20.

Dependence of the Thermodynamics of Urea-induced Unfolding on the Concentration of Osmolyte—Fluorescence- and far-UV CD-monitored urea-induced unfolding transitions, such as those in Fig. 1 (*a*, *b*, *d* and *e*), were determined at different concentrations of TMAO and sarcosine in the range 0–1 M. Fig. 2 shows the dependence of the free energy of unfolding, $\Delta G_{\text{UN}}^{\text{f}}$; the preferential free energy of interaction of urea with U as compared to with N , m_{UN} ; and the mid-point of the transition, C_{m} , on the concentration of TMAO and sarcosine. At any one concentration of osmolyte, the value of any of these thermodynamic parameters is essentially the same for both osmolytes. The free energy of unfolding is seen to increase linearly from a

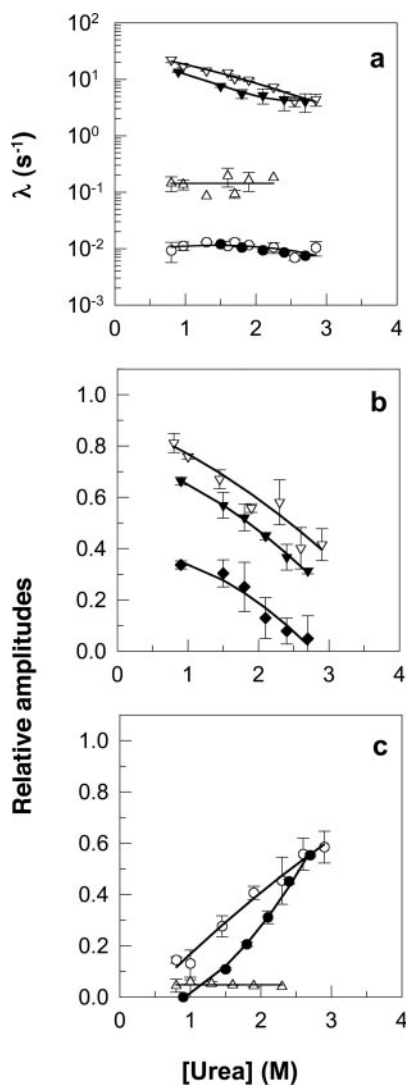


FIG. 5. Urea dependence of the folding kinetics at pH 8, 25 °C, in the absence of any osmolyte. *a*, the dependence of the logarithm of each of the folding rates on urea concentration in the absence of any osmolyte: fast refolding rate constant, λ_2 (∇), slow refolding constant, λ_1 (\circ), and intermediate refolding rate constant, λ_3 (Δ), monitored by fluorescence at 320 nm; and fast refolding rate constant, λ_2 (\blacktriangledown) and slow refolding constant, λ_1 (\bullet) monitored by CD at 222 nm. *b*, the dependences on the concentration of urea of the relative amplitude (α_2) of the fast phase of refolding, from fluorescence (∇) and from CD (\blacktriangledown) are shown. The dependence of the relative amplitude (α_4) of the burst phase of refolding (\blacklozenge) monitored by CD is also shown. *c*, the dependence on urea concentration of the relative amplitude (α_1) of the slow phase of refolding from fluorescence (\circ) and from CD (\bullet) and the urea dependence of the relative amplitude (α_3) of the intermediate phase of refolding in the absence of any osmolyte from fluorescence (Δ) is shown in *c*. The fluorescence data in *a* have been borrowed from Fig. 7 in Ref. 20. In all of the panels, the error bars represent the standard deviations obtained from three repetitions of the experiment, and the continuous lines through the data have been drawn by inspection only.

value of $4.7 (\pm 0.1)$ kcal mol $^{-1}$ in the absence of osmolyte to a value of $7.0 (\pm 0.1)$ kcal mol $^{-1}$ in 1 M TMAO or 1 M sarcosine. The value of m_{UN} is $-1.16 (\pm 0.04)$ kcal mol $^{-1}$ M $^{-1}$ in the absence of osmolyte and remains unchanged with the increase in concentration of TMAO or sarcosine up to 1 M; the values at all concentrations of TMAO and sarcosine are within three standard deviations of the value obtained in the absence of osmolyte, in support of the assumptions made in Equation 3. The linear dependence of the free energy of unfolding on the concentration of TMAO and sarcosine was fit to Equation 2, which yielded a value of 2.42 kcal mol $^{-1}$ M $^{-1}$ for $m_{UN}^N(\text{TMAO})$,

the preferential free energy of interaction of TMAO with N as compared to with U , and a value of 2.33 kcal mol $^{-1}$ M $^{-1}$ for $m_{UN}^N(\text{sarcosine})$, the preferential free energy of interaction of sarcosine with N as compared to with U .

Kinetics of Refolding in the Absence and Presence of Osmolytes—The refolding of urea-unfolded barstar has been described as a three-exponential process when monitored by fluorescence (20). The relative amplitude of the intermediate phase is less than 5% of the total refolding amplitude at all concentrations of urea. For describing the kinetics of refolding in the presence of 1 M TMAO and 1 M sarcosine, it also became essential to include this additional intermediate phase. Panels *a–c* in Fig. 3 show that in the absence of osmolyte and in the presence of 1 M TMAO and 1 M sarcosine, the fast rate of refolding increases with a decrease in the concentration of urea, when monitored by intrinsic tryptophan fluorescence. Panels *d–f* in Fig. 3 likewise show that the fast rate of refolding increases with a decrease in the concentration of urea in the absence and presence of 1 M TMAO and 1 M sarcosine, when monitored by CD. When measured by CD, the refolding of urea-unfolded barstar in the absence and in the presence of 1 M TMAO or 1 M sarcosine is described as a two-exponential process. In 0.9 M urea, the rates of the fast phase of refolding in 1 M TMAO (29 ± 2 s $^{-1}$ by fluorescence and 22 ± 1 s $^{-1}$ by CD) and 1 M sarcosine (32 ± 2 s $^{-1}$ by fluorescence and 25 ± 1 s $^{-1}$ by CD) are faster than the rate in the absence of osmolyte (20 ± 3 s $^{-1}$ by fluorescence and 13 ± 1 s $^{-1}$ by CD). Sarcosine absorbs highly in the far-UV region, and so the data obtained for refolding of barstar in the presence of sarcosine are noisy despite many traces being averaged. In the presence of the osmolyte at low denaturant concentrations, a significant fraction of the folding reaction is too fast to be observed so that significant changes in fluorescence and CD signals occur in a submillisecond burst phase.

Burst Phase Changes in Fluorescence and Far-UV CD during Folding—The occurrence of a burst change in fluorescence, for folding in 1 M TMAO and 1 M sarcosine but not in the absence of osmolyte, is illustrated in Fig. 4 (*a–c*), where the kinetic amplitudes of folding are compared with equilibrium amplitudes over a range of urea concentrations in the pretransition zone. In all cases, the end points, $t = \infty$, of the kinetic refolding curves fall on the equilibrium unfolding curves, indicating that each folding reaction has been monitored to completion. In the absence of any osmolyte, the start points at $t = 0$ of the kinetic curves for refolding, obtained by extrapolation of the fits to the observed kinetic curves, fall on the linearly extrapolated unfolded protein base line. For refolding in 1 M TMAO and 1 M sarcosine, the $t = 0$ points of the kinetic refolding curves do not fall on the linearly extrapolated unfolded protein base lines; these $t = 0$ points show an apparently sigmoidal dependence on the concentration of urea.

The occurrence of a burst phase change in far-UV CD, for folding in the absence of any osmolyte in the presence of 1 M TMAO and in the presence of 1 M sarcosine is best illustrated in Fig. 4 (*d–f*), where the kinetic amplitudes of folding are compared with equilibrium amplitudes over a range of urea concentrations in the pretransition zone. In all cases, the end points, $t = \infty$, of the kinetic refolding curves fall on the equilibrium unfolding curves, indicating that each folding reaction has been monitored to completion. In the absence of any osmolyte, as well as in the presence of 1 M TMAO and 1 M sarcosine, the start points at $t = 0$, of the kinetic curves for refolding, obtained by extrapolation of the fits to the observed kinetic curves, do not fall on the linearly extrapolated unfolded protein base lines but appear to show a sigmoidal dependence on the concentration of urea.

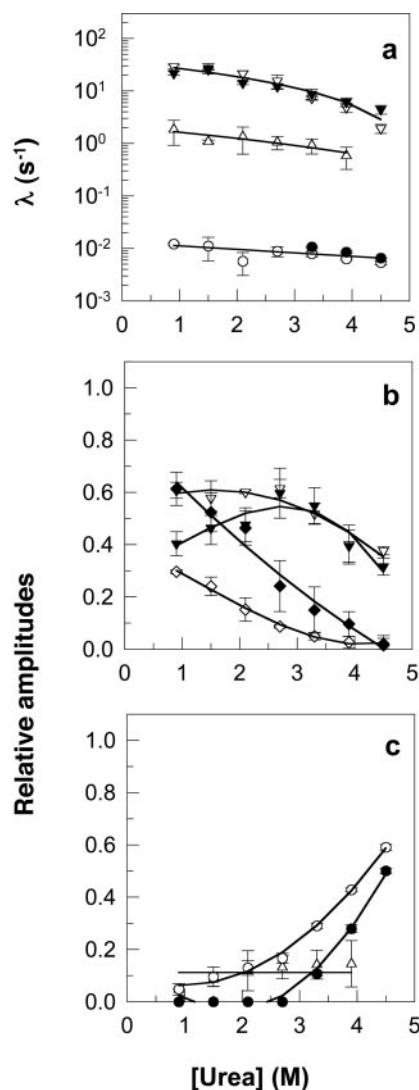


FIG. 6. Urea dependence of the folding kinetics at pH 8, 25 °C, in the presence of 1 M TMAO. *a*, the dependence of the logarithm of each of the folding rates on the concentration of urea in 1 M TMAO: fast refolding rate constant, λ_2 (∇), slow refolding constant, λ_1 (\circ), and intermediate refolding rate constant, λ_3 (Δ), monitored by fluorescence at 320 nm; and fast refolding rate constant, λ_2 (\blacktriangledown) and slow refolding constant, λ_1 (\bullet) monitored by far-UV CD at 222 nm. *b*, the dependence on the concentration of urea of the relative amplitude (α_2) of the fast phase of refolding, from fluorescence (∇) and from CD (\blacktriangledown) are shown. The dependence of the relative amplitude (α_4) of the burst phase of refolding, from fluorescence (\diamond) and from CD (\blacklozenge), are also shown. The dependence on the concentration of urea of the relative amplitude (α_1) of the slow phase of refolding, from fluorescence (\circ) and from CD (\bullet) and the urea dependence of the relative amplitude (α_3) of the intermediate phase of refolding in from fluorescence (Δ) are shown in *c*. In all of the panels, the *error bars* represent the standard deviations obtained from three repetitions of the experiment, and the *continuous lines* through the data have been drawn by inspection only.

For folding in the absence or presence of osmolyte, there is an insignificant burst phase change in CD in marginally stabilizing yet native conditions, at urea concentrations just preceding the start of the folding transition zone in agreement with earlier reports (33, 40). A burst phase of less than 10%, within the estimated 10% error of determination (see “Experimental Procedures”) is seen at 2.4 M urea (which is equivalent to 1.0 M guanidine hydrochloride in which no burst phase was observed earlier (33)). At lower urea concentrations, the relative burst phase is seen to increase and shows a sigmoidal dependence, suggesting the presence of secondary structure in the product

of the burst phase, I_E , at a few milliseconds of folding, under more stabilizing conditions, as reported earlier (40).

To determine whether the sigmoidal dependences of the $t = 0$ points on urea concentration, shown in Fig. 4, represent two-state transitions between the unfolded form in the refolding conditions and I_E , the data were fit to Equation 9. Equation 9 assumes a two-state transition in which the free energy of unfolding of I_E in the presence of urea and osmolyte, $\Delta G_{UI}^{\text{III}}$, has a linear dependence on urea concentration (with a slope m_{UI}) as well as on osmolyte concentration (with slope m_O^I). For CD-monitored folding in the absence of osmolyte (Fig. 4*d*), the values obtained for ΔG_{UI} and m_{UI} agree with previously determined values (20). For folding data obtained in the presence of either 1 M TMAO (Fig. 4, *b* and *e*) or 1 M sarcosine (Fig. 4, *c* and *f*), it was not possible to obtain values for ΔG_{UI} , m_{UI} , and m_O^I that satisfied both the fluorescence and CD data. The values for the parameters obtained from the fits are listed in the legend to Fig. 4. It is seen that the values obtained for ΔG_{UI} and m_{UI} for folding in the presence of osmolyte are similar to the values obtained in the absence of osmolyte. For each osmolyte, however, the value obtained for m_O^I from CD and fluorescence measurements are very different. These results suggest that the transition from the unfolded state in refolding conditions to I_E is not two-state.

Urea Dependence of the Observable Kinetics in the Absence and Presence of 1 M Osmolyte—Panels *a–c* in Fig. 5 show the rates and relative amplitudes of the observable kinetic phases of folding, in the absence of osmolyte, measured both by fluorescence and by far-UV CD. Panels *a–c* in Fig. 6 do likewise for folding in the presence of 1 M TMAO, and panels *a–c* in Fig. 7 do likewise for folding in the presence of 1 M sarcosine. Data for fluorescence-monitored kinetics in the absence of any osmolyte (Fig. 5) have been taken from an earlier report (20).

A comparison of Figs. 5*a*, 6*a*, and 7*a* indicates that: (i) In the absence of the osmolyte, the observed fast rate constant for folding monitored by fluorescence is faster than the fast rate constant obtained from monitoring far-UV CD at any concentration of urea. Such a difference had been observed earlier also (33) for folding in 1 M guanidine HCl. (ii) The observed fast rate constants for folding in the presence of 1 M TMAO or 1 M sarcosine are essentially the same whether determined by CD or fluorescence measurements. (iii) The rate constant of the fast phase of folding, which represents the folding of I_E to I_L , increases at any concentration of urea studied, upon the addition of 1 M TMAO or 1 M sarcosine, whether monitored by fluorescence or CD measurement, because the stabilization of I_E by osmolytes leads to greater accumulation of I_E . (iv) The curvature (roll over) in the folding arm of the chevron is more pronounced for folding in the presence of 1 M TMAO or 1 M sarcosine than in the absence of osmolyte, when monitored by either probe; because the stabilization of I_E by osmolyte has a larger effect at lower urea concentrations. Such rollovers in the refolding arms of chevrons have been observed for many proteins (41, 42), including barstar (20, 32) at low concentrations of urea, where transient folding intermediates become sufficiently stable to populate to significant extents. (v) The folding arm of the chevron for the fast rate constant appears to be shifted horizontally to higher concentrations of urea, in the presence of 1 M TMAO or 1 M sarcosine. (vi) The slow rate constant for folding is not altered at any urea concentration by the presence of 1 M TMAO or 1 M sarcosine. (vii) The rate constant of the intermediate phase (fluorescence data only) is no longer independent of the concentration of urea in the presence of 1 M TMAO or 1 M sarcosine, as it is in the absence of osmolyte.

A comparison of the relative amplitudes of the observable

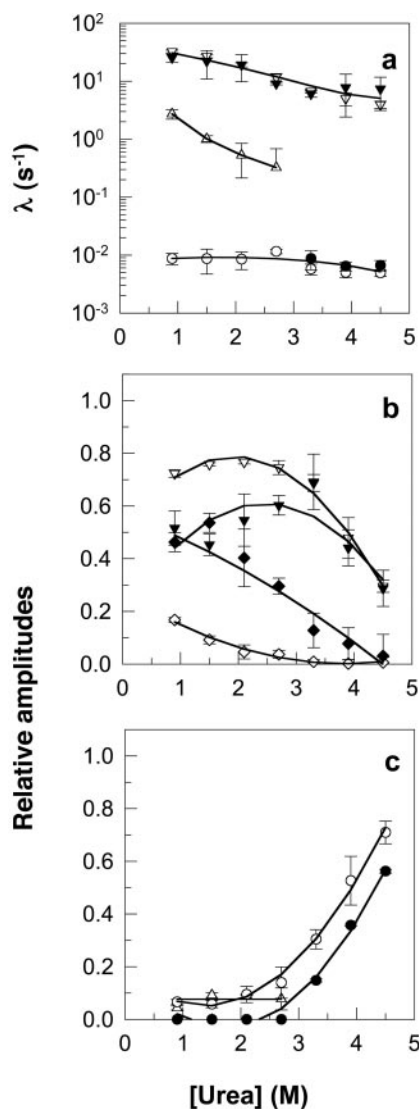


FIG. 7. Urea dependence of the folding kinetics at pH 8, 25 °C, in the presence of 1 M sarcosine. *a*, the dependence of the logarithm of each of the folding rates on urea concentration, in 1 M sarcosine: fast refolding rate constant, λ_2 (∇), slow refolding constant, λ_1 (\circ), and intermediate refolding rate constant, λ_3 (Δ), monitored by fluorescence at 320 nm; and fast refolding rate constant, λ_2 (\blacktriangledown) and slow refolding constant, λ_1 (\bullet) monitored by far-UV CD at 222 nm. *b*, the dependences on urea concentration of the relative amplitude (α_2) of the fast phase of refolding in 1 M sarcosine, (∇) from fluorescence, and (\blacktriangledown) from CD are shown. The dependences of the relative amplitude (α_4) of the burst phase of refolding, from fluorescence (\diamond) and from CD (\blacklozenge) are also shown. *c*, the dependence on urea concentration of the relative amplitude (α_1) of the slow phase of refolding in, from fluorescence (\circ) and from CD (\bullet) and the urea dependence of the relative amplitude (α_3) of the intermediate phase of refolding from fluorescence (Δ) are shown. In all of the panels, the error bars represent the standard deviations obtained from three repetitions of the experiment, and the continuous lines through the data have been drawn by inspection only.

phases for folding in the pretransition zone in the absence and presence of osmolyte (Fig. 5, *b* and *c*; Fig. 6, *b* and *c*; and Fig. 7, *b* and *c*) indicates that: (i) The relative amplitudes of the fast phase as well as of the slow phase are less at lower urea concentrations when monitored by far-UV CD than when monitored by fluorescence, because of the presence of a burst phase and the absence of the intermediate phase in the CD measurements (see “Experimental Procedures”). (ii) At the lowest concentration of urea (0.9 M), the relative burst phase amplitude for refolding in the absence of osmolyte is 34% when monitored by far-UV CD, whereas no burst phase is seen in fluorescence

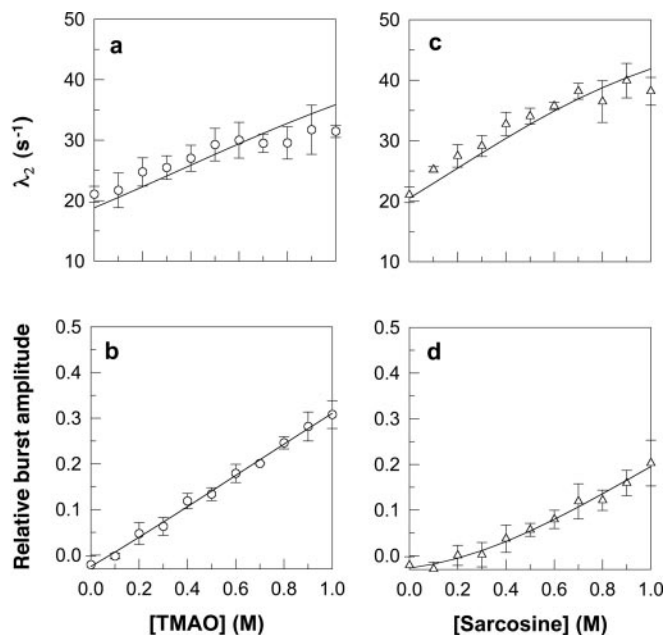


FIG. 8. Dependence of fast refolding rates and burst phase amplitudes on osmolyte concentration. The refolding of the protein in 0.9 M urea at pH 8, 25 °C, was monitored by fluorescence at 320 nm. *a*, dependence of fast refolding rate constant, λ_2 , on TMAO concentration. The continuous line through the data is drawn according to Equation 11 with values for k^0 , m_k^D , m_k^O , ΔG_{UI} , m_{UI} , and m_O^I of 50 s⁻¹, 0 M⁻¹, 0 M⁻¹, 0.55 kcal mol⁻¹, -0.94 kcal mol⁻¹ M⁻¹, and 0.85 kcal mol⁻¹ M⁻¹, respectively. *b*, dependence of the relative amplitude of the burst phase, α_4 , on the concentration of TMAO. The continuous line through the dependence on the concentration of TMAO is drawn according to Equation 9, with values of ΔG_{UI} , m_{UI} , and m_O^I (TMAO) of 0.5 kcal mol⁻¹, -0.99 kcal mol⁻¹ M⁻¹, and 0.85 kcal mol⁻¹ M⁻¹, respectively. *c*, dependence of fast refolding rate constant, λ_2 , on sarcosine concentration. The continuous line through the data is drawn according to Equation 11 with values for k^0 , m_k^D , m_k^O , ΔG_{UI} , m_{UI} , and m_O^I of 50 s⁻¹, 0 M⁻¹, 0 M⁻¹, 0.55 kcal mol⁻¹, -0.85 kcal mol⁻¹ M⁻¹, and 1.19 kcal mol⁻¹ M⁻¹, respectively. *d*, dependence of the relative amplitude of the burst phase, α_4 , on the concentration of sarcosine during refolding in 0.9 M urea. The continuous line through the dependence on the concentration of sarcosine is drawn according to Equation 9, with values of ΔG_{UI} , m_{UI} , and m_O^I (sarcosine) of 0.55 kcal mol⁻¹, -0.95 kcal mol⁻¹ M⁻¹, and 1.15 kcal mol⁻¹ M⁻¹, respectively. The error bars on the data points are standard deviations from three separate determinations.

measurements. (iii) At the lowest concentration of urea (0.9 M), the relative burst phase amplitude for refolding in 1 M TMAO monitored by CD is as high as 60% as opposed to 30% when monitored by fluorescence, and the relative burst phase amplitude for refolding in 1 M sarcosine monitored by CD is 50% as opposed to 17% when monitored by fluorescence. (iv) In the absence of osmolyte, the slow phase of folding is not observed in CD-monitored kinetics studies when refolding is carried out in concentrations of urea below 0.9 M. (v) In the presence of 1 M TMAO or 1 M sarcosine, the slow phase of folding is not observed in CD-monitored kinetics studies for urea concentrations below 2.7 M. (vi) The relative amplitude of the fast phase of refolding in the presence of 1 M TMAO or 1 M sarcosine is less at lower concentrations of urea because of either the additional burst phase (when monitored by fluorescence) or enhanced amplitudes of the burst phase (when monitored by CD). (vii) The relative amplitude of the slow phase of refolding in the presence of 1 M TMAO or 1 M sarcosine is less at all concentrations of urea in the pretransition zone when monitored by either probe.

Dependence of Refolding Kinetics Measured by Fluorescence on Osmolyte Concentration—Fig. 8*a* shows the dependence of the observed rate constant of the fast phase of refolding in 0.9 M urea on the concentration of TMAO, and Fig. 8*c* does likewise

for the dependence on the concentration of sarcosine. In both cases, the dependence on osmolyte concentration can be well accounted for by Equation 11 (see the legend to Fig. 8), supporting the assumption of Equation 2 that the degree of stabilization of I_E is dependent linearly on the concentration of osmolyte added.

The dependence of the relative amplitude of the burst phase change in fluorescence, which occurs during refolding in 0.9 M urea, on the concentration of TMAO (Fig. 8*b*), as well as on the concentration of sarcosine (Fig. 8*d*), is well described by Equation 9 with values for ΔG_{UI} , m_{UI} , and m_{UI}^1 (TMAO) of 0.51 kcal mol⁻¹, -0.99 kcal mol⁻¹ M⁻¹, and 0.85 kcal mol⁻¹ M⁻¹, respectively, and ΔG_{UI} , m_{UI} , and m_{UI}^1 (sarcosine) of 0.55 kcal mol⁻¹, -0.95 kcal mol⁻¹ M⁻¹, and 1.15 kcal mol⁻¹ M⁻¹, respectively (see the legend to Fig. 8). These values are similar to those obtained from the dependence of the fast rate constant on the concentrations of TMAO and sarcosine in 0.9 M urea (Fig. 8, *a* and *c*) or from the dependence of the burst phase change in fluorescence on the concentration of urea for refolding in 1 M TMAO and in 1 M sarcosine (Fig. 4, *b* and *c*).

The apparent rate constants of the intermediate and slow phases of refolding in 0.9 M urea are independent of the concentration of TMAO or sarcosine (data not shown). The relative amplitude of the fast phase of refolding in 0.9 M urea decreases with an increase in concentration of TMAO and sarcosine at the expense of the increase in burst phase amplitude. The relative amplitudes of the slow and intermediate phases are essentially independent of TMAO and sarcosine concentrations (data not shown).

DISCUSSION

Mechanism of Osmolyte-induced Stabilization of Barstar: a General Counteracting Mechanism—TMAO and sarcosine stabilize the native state of barstar (Fig. 1). The observation that ΔG_{UN}^0 increases linearly with an increase in the concentration of the osmolyte (Fig. 2) validates the use of the weak interaction model for describing the interactions of these osmolytes with barstar. In another study, it had been shown that the free energy of unfolding of both barnase and the Notch ankyrin domain depends linearly on TMAO concentration and that its sensitivity to urea is independent of the presence of TMAO (43), again confirming that urea and TMAO exert independent effects that are additive.

Counteracting osmolytes consist of the methylamine class of osmolytes and have the special ability to protect intracellular proteins against the inactivating effects of urea (44, 45). Urea-containing organs like mammalian kidneys contain betaine and glycerophosphocholine as counteracting osmolytes; cartilaginous fishes and the coelacanth contain TMAO as the counteracting osmolyte in their urea-rich cells (46–50). Cartilaginous fish and the coelacanth have intracellular concentrations of urea as high as 0.6 M, and their intracellular levels of TMAO are roughly half that of urea (49, 51, 52). It is seen here (Fig. 2) that in the stabilization of barstar by TMAO and sarcosine, the values of m_{UN} (-1.16 ± 0.04 kcal mol⁻¹ M⁻¹), m_{UN}^0 (sarcosine) (2.33 kcal mol⁻¹ M⁻¹), and m_{UN}^0 (TMAO) (2.42 kcal mol⁻¹ M⁻¹) are such that when TMAO and urea, or sarcosine and urea, are present in concentrations with the ratio 1:2, the osmolyte and denaturant offset the effect of each other. The observation that the ratio of concentrations of urea and osmolyte that offset each other's action on barstar, a protein that has not evolved in the presence of these osmolytes, is the same as that found for proteins that have evolved in their presence indicates that the ability of organic osmolytes to protect against denaturation of proteins is generic and independent of evolutionary history (1, 2, 53).

Osmolytes Do Not Alter the Basic Folding Mechanism—A comparison of the folding kinetics in the absence and in the presence of 1 M TMAO or 1 M sarcosine (Figs. 5–7) indicates that the basic folding mechanism of barstar (Scheme 1) is unaffected by the presence of osmolyte. Most effects caused by TMAO or sarcosine, including the observation that the fast folding rates are accelerated, can be accounted for either by the increase in the stability of the native state (Fig. 2) or by invoking an increase in the stability, and an alteration in the structure of the early folding intermediate I_E (Scheme 1). The use of osmolytes to perturb the stabilities of intermediates on the folding pathway has not only allowed the effects of osmolytes on a folding pathway to be elucidated, but it has also allowed several fundamental features of the folding reaction of barstar to be clarified. The effects of the two osmolytes on structure formation during folding, particularly on the structural heterogeneity of the early intermediate I_E , are discussed below.

Initial Collapse of the Polypeptide Chain—Early fluorescence resonance energy transfer as well as 8-anilino-1-naphthalene-sulfonic acid binding studies had indicated that the polypeptide chain of barstar collapses to a compact form within the initial few milliseconds of refolding in low as well as in marginally destabilizing concentrations of denaturant (14, 33), suggesting that (i) the collapse reaction must have brought together hydrophobic residues to form exposed hydrophobic patches capable of binding 8-anilino-1-naphthalene-sulfonic acid (14, 33) and (ii) the collapse must occur not only in strongly stabilizing but also in marginally stabilizing conditions for folding, as well. The collapse reaction was, however, observed not to be accompanied by any change in fluorescence (20, 24, 31), as also seen here in both the absence (Fig. 4*a*) and the presence of osmolytes (Fig. 4, *b* and *c*), indicating that the tryptophan residues in the product of the collapse reaction are as hydrated as they are in *U*. In marginally stabilizing conditions (in the presence of 1 M guanidine HCl), the product of the collapse reaction was found to be devoid of significant helical secondary structure (33). This was the first detection of a structure-less globule as the product of the initial hydrophobic collapse during the folding of any protein. For several other proteins, including BBL (54), cytochrome *c* (18), and CspB (55), the initial collapse reaction has also been shown to precede formation of any specific structure and to occur in the nanosecond to microsecond time domain. Lattice model simulations of folding (23) have also suggested that folding proceeds through an obligatory, rapidly collapsed, structure-less globule (56–58). In the case of barstar, an equilibrium model (59, 60), which was developed to describe the initial events that occur during folding, also indicates that the initial collapse reaction, which occurs through progressively more compact forms, as seen for homopolymers (61), precedes specific structure formation. Thus, it is also likely that collapse of *U* to the structure-less globule, U_C , has occurred well before the product is observed at a few milliseconds. Fortuitously, U_C remains populated even at a few milliseconds after commencement of folding in conditions that confer only marginal stability, because in such conditions subsequent folding reactions of U_C do not occur to any significant extent in the first few milliseconds after collapse. Here, it is seen that U_C remains devoid of specific secondary structure even in the presence of 1 M osmolyte when the stabilizing effect of the osmolyte is countered by the destabilizing effect of 4.5 M urea (Fig. 5).

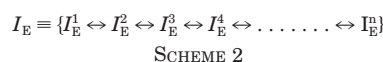
Formation of the Specific Early Intermediate, I_E —When the folding of barstar is carried out under strongly stabilizing conditions, at low urea concentrations, a burst phase change in far-UV CD is observed at a few milliseconds of refolding, indicating the formation of some helical secondary structure. It therefore appears that at a few milliseconds of folding under

strongly stabilizing conditions, U_C has transformed to an intermediate with specific structure. This intermediate with specific structure is the early intermediate I_E . Specific structure in I_E had been identified earlier in fluorescence-monitored kinetic studies (20) of folding in the presence of stabilizing salt, in which the fluorescence emission spectrum of I_E was found to be distinct from that determined in the absence of the stabilizing salt. The secondary structure content of I_E appears to depend on the concentration of urea in which folding is carried out (Fig. 4). Given that a pre-equilibrium is established between U_C and I_E at a few milliseconds of folding, because the subsequent folding of I_E to I_L is much slower, the dependence on urea concentration of the secondary structural content of I_E represents the dependence on urea concentration of the equilibrium constant of the U_C and I_E pre-equilibrium. Thus, both U_C and I_E are populated at a few milliseconds of folding, but their relative proportions depend on the concentration of urea present. Both U_C and I_E are compact; 8-anilino-1-naphthalene-sulfonic acid binding occurs within a few milliseconds of the commencement of folding over the entire range of denaturant concentration (14). In the absence of added osmolyte, both U_C and I_E are U -like in their fluorescence properties. They are distinguished only in I_E possessing 30% of the N state far-UV CD (in the absence of osmolyte), whereas U_C is U -like in its far-UV CD properties.

Folding Studies in the Presence of Osmolyte Indicate that the Formation of I_E Is a Multi-step Process—A simple test has been carried out to determine whether the pre-equilibrium that is established between U_C and I_E within the initial few milliseconds of folding, is two-state. If the transition is indeed two-state, then the same values should be obtained for the thermodynamic parameters characterizing the $U_C \rightleftharpoons I_E$ transition, whether the transition is probed by fluorescence or far-UV CD measurements. In the absence of osmolyte, it was not possible to obtain values for ΔG_{UI} and m_{UI} from fluorescence measurements in the presence of different concentrations of urea, because of the absence of a burst phase change in fluorescence. In far-UV CD measurements, burst phase changes were observed at low urea concentrations, and these could be analyzed to yield values for ΔG_{UI} and m_{UI} . But for folding in the presence of either TMAO or sarcosine, burst phases were observed in both fluorescence and far-UV CD measurements. In either case, the dependence of the amplitude of the burst phase change on urea was fit to Equation 9, which describes the $I_E \rightleftharpoons U_C$ reaction as a two-state pre-equilibrium. It was found to be impossible to obtain the same set of values for ΔG_{UI} , m_{UI} , and m_O^I that would satisfy the fits of the fluorescence as well as the CD data, for folding in the presence of either 1 M TMAO or 1 M sarcosine (see legend to Fig. 4). The $U_C \rightleftharpoons I_E$ transition cannot therefore be described as a two-state transition, either in the absence or presence of osmolyte. In the presence of either osmolyte, I_E appears to comprise at least two structurally distinct components that differ in their fluorescence and far-UV CD properties.

Osmolytes Alter the Structure of I_E —It is instructive to examine how the optical properties of I_E vary upon addition of osmolyte. These optical properties are determined from the amplitudes of the burst phase changes that occur at the lowest urea concentration in the absence and presence of osmolyte (Fig. 4). In 0.9 M urea in the absence of osmolyte, I_E is U -like in its fluorescence but possesses about 30% of the native state far-UV CD. Upon the addition of 1 M TMAO, I_E is found to possess about 30% of the native state fluorescence and about 60% of the native state far-UV CD. Upon the addition of 1 M sarcosine, I_E is found to possess about 20% of the native state fluorescence and about 50% of the native state far-UV CD.

These results indicate that I_E is composed of different structural forms in equilibrium with each other.



In 0.9 M urea in the absence of osmolyte, I_E^1 is populated predominantly, and hence the properties determined for I_E (compactness (14, 33), U -like fluorescence, 30% of native state far-UV CD) reflect mainly the properties of I_E^1 . In 0.9 M urea in the presence of 1 M TMAO, the equilibrium within I_E appears to be shifted so that I_E^2 is populated predominantly, and hence, the properties determined for I_E in 0.9 M urea and 1 M TMAO (compactness, 30% of native state fluorescence, 60% of native state far-UV CD) reflect properties of I_E^2 . In the presence of 1 M sarcosine, I_E^3 is populated predominantly so that the properties determined for I_E in 1 M sarcosine (compactness, 20% of native state fluorescence, 50% of native state far-UV CD) reflect mainly the properties of I_E^3 . In this way, the optical properties of I_E depend on the conditions of refolding, suggesting that I_E is structurally distinct in each of the conditions chosen for refolding.

Perturbation of Structure in the I_E Ensemble by Osmolytes—It is apparent that I_E consists of many different forms, some less structured and some more structured, and that in the absence of osmolyte, the less structured forms are thermodynamically favored. The ability of TMAO as well as sarcosine to perturb the equilibria existing between the different members of I_E and in this way determine the structure of I_E , suggests that the different structural components differ in the extent of exposed surface area that is hydrated preferentially in the presence of either osmolyte. In the presence of osmolyte, when hydrophobic interactions are strengthened because of preferential exclusion, more structured members of the I_E ensemble are favored thermodynamically, and the degree of formation and stabilization of structure is dependent on the specific osmolyte present. A qualitative indication of how the members of the I_E ensemble differ in the extent of exposed surface area hydrated preferentially in the presence of osmolyte becomes apparent from consideration of values determined for m_O^I , the preferential free energy of interaction of the osmolyte with U relative to with I_E . The value of m_O^I/m_O^N is a measure of the degree of preferential hydration of I and serves as a measure of the progress of the folding reaction. In the presence of 1 M TMAO, m_O^I/m_O^N has a value of $0.85/2.4 = 0.354$ when determined from the fluorescence-monitored kinetic studies, but has a value of $1.9/2.4 = 0.792$ when determined by CD-monitored kinetic studies. In the presence of 1 M sarcosine, m_O^I/m_O^N has a value of $1.15/2.4 = 0.479$ when determined from fluorescence measurements and has a value of $2.1/2.4 = 0.875$ when determined from CD measurements. Widely disparate extents of the progress of the folding reaction that is achieved upon the formation of I_E are therefore obtained when different probes are used to monitor the reaction.

Implications of the Structure-modulating Capability of an Osmolyte—The observation that different structural components in I_E can be stabilized differentially in the presence of different osmolytes implies that different folding pathways will dominate in the presence of different osmolytes. In the absence of osmolyte but at low urea concentrations, I_E is compact with significant secondary structure but appears to possess a fully solvated core (its fluorescence is U -like). In the presence of osmolyte it not only has considerably more secondary structure, but its core appears to be partially consolidated (its fluorescence is no longer U -like). The extent to which structure is induced depends on the nature of the osmolyte. In the strongly stabilizing conditions provided by the osmolyte, I_E is compact

with significant structure and hence appears to be the product of a specific folding reaction. A multi-site, time-resolved fluorescence resonance energy transfer characterization (35) of the slow folding reaction has also indicated that different pathways dominate under different folding conditions, when different components of the late intermediate I_L are stabilized under different conditions. Very recently, a comparative study of the folding of barstar in urea and guanidine HCl has suggested that different folding pathways are utilized in the two denaturants (29). Taken together, these results indicate that for the folding of any protein, different folding pathways will appear to be operative under different folding conditions and that osmolytes may channel folding along particular pathways by preferentially stabilizing one or more structural components of an intermediate ensemble populated on that pathway.

Acknowledgments—We thank members of our laboratory for discussion and B. Rami for comments on the manuscript.

REFERENCES

- Yancey, P. H., Clark, M. E., Hand, S. C., Bowlus, R. D., and Somero, G. N. (1982) *Science* **217**, 1214–1222
- Brown, A. D., and Simpson, J. R. (1972) *J. Gen. Microbiol.* **72**, 589–591
- Hochachka, P. W., and Somero, G. N. (1984) in *Water-solute Adaptations: The Evolution and Regulation of Biological Solutions*, pp. 304–354, Princeton University Press, Princeton, NJ
- Arakawa, T., and Timasheff, S. N. (1985) *Biophys. J.* **47**, 411–414
- Timasheff, S. N. (1992) in *Water and Life: A Comparative Analysis of Water Relationships at the Organismic, Cellular and Molecular Levels* (Somero, G. N., Osmond, C. B., and Bolis, C. L., eds) pp. 70–84, Springer-Verlag, Berlin, Germany
- Timasheff, S. N. (1993) *Annu. Rev. Biophys. Biomol. Struct.* **22**, 67–97
- Schellman, J. A. (1990) *Biophys. Chem.* **37**, 121–140
- Liu, Y., and Bolen, D. W. (1995) *Biochemistry* **34**, 12884–12891
- Wang, A., and Bolen, D. W. (1997) *Biochemistry* **36**, 9101–9108
- Baskakov, I., and Bolen, D. W. (1998) *J. Biol. Chem.* **273**, 4831–4834
- Uversky, V. N., Li, J., and Fink, A. L. (2001) *FEBS Lett.* **509**, 31–35
- Russo, A. T., Rosgen, J., and Bolen, D. W. (2003) *J. Mol. Biol.* **330**, 851–866
- Melo, E. P., Chen, L., Cabral, J. M., Fojan, P., Petersen, S. B., and Otzen, D. E. (2003) *Biochemistry* **42**, 7611–7617
- Shastri, M. C. R., and Udgaonkar, J. B. (1995) *J. Mol. Biol.* **247**, 1013–1027
- Houry, W. A., Rothwarf, D. M., and Scheraga, H. A. (1996) *Biochemistry* **35**, 10125–10133
- Houry, W. A., and Scheraga, H. A. (1996) *Biochemistry* **35**, 11734–11746
- Morgan, C. L., Miranker, A., and Dobson, C. M. (1998) *Biochemistry* **37**, 8473–8480
- Akiyama, S., Takahashi, S., Ishimori, K., and Morishima, I. (2000) *Nat. Struct. Biol.* **7**, 514–520
- Nishimura, C., Jane Dyson, H., and Wright, P. (2002) *J. Mol. Biol.* **322**, 483–489
- Pradeep, L., and Udgaonkar, J. B. (2002) *J. Mol. Biol.* **324**, 331–347
- Georgescu, R. E., Li, J. H., Goldberg, M. E., Tasayco, M. L., and Chaffotte, A. F. (1998) *Biochemistry* **37**, 10286–10297
- Dill, K. A., and Chan, H. S. (1997) *Nat. Struct. Biol.* **4**, 10–19
- Dinner, A. R., Sali, A., Smith, L. J., Dobson, C. M., and Karplus, M. (2000) *Trends Biochem. Sci.* **25**, 331–339
- Dobson, C. M., Sali, A., and Karplus, M. (1998) *Angew. Chem. Int. Ed.* **37**, 868–893
- Onuchic, J. N., Luthey-Schulten, Z., and Wolynes, P. G. (1997) *Annu. Rev. Phys. Chem.* **48**, 545–600
- Zaidi, F. N., Nath, U., and Udgaonkar, J. B. (1997) *Nat. Struct. Biol.* **4**, 1016–1024
- Goldbeck, R. A., Thomas, Y. G., Chen, E., Esquerra, R. M., and Klinger, D. S. (1999) *Proc. Natl. Acad. Sci. U. S. A.* **96**, 2782–2787
- Juneja, J., and Udgaonkar, J. B. (2002) *Biochemistry* **41**, 2641–2654
- Sridevi, K., and Udgaonkar, J. B. (2002) *Biochemistry* **41**, 1568–1578
- Wright, C. F., Lindorff-Larsen, K., Randles, L. G., and Clarke, J. (2003) *Nat. Struct. Biol.* **10**, 658–662
- Shastri, M. C. R., Agashe, V. R., and Udgaonkar, J. B. (1994) *Protein Sci.* **3**, 1409–1417
- Schreiber, G., and Fersht, A. R. (1993) *Biochemistry* **32**, 11195–11203
- Agashe, V. R., Shastri, M. C. R., and Udgaonkar, J. B. (1995) *Nature* **377**, 754–757
- Bhuyan, A. K., and Udgaonkar, J. B. (1999) *Biochemistry* **38**, 9158–9168
- Sridevi, K., Lakshminanth, G., Krishnamoorthy, G., and Udgaonkar, J. B. (2004) *J. Mol. Biol.* **337**, 699–711
- Khurana, R., and Udgaonkar, J. B. (1994) *Biochemistry* **33**, 106–115
- Schellman, J. A. (1987) *Annu. Rev. Biophys. Biophys. Chem.* **16**, 115–137
- Timasheff, S. N. (1998) *Adv. Protein Chem.* **51**, 355–432
- Agashe, V. R., and Udgaonkar, J. B. (1995) *Biochemistry* **34**, 3286–3299
- Nolting, B., Golbik, R., Soler-Gonzalez, A. S., and Fersht, A. R. (1997) *Biochemistry* **36**, 9899–9905
- Yamasaki, K., Ogasahara, K., Yutani, Y., Oobatake, M., and Kanaya, S. (1995) *Biochemistry* **34**, 16552–16561
- Parker, M. J., and Marqusee, S. (1999) *J. Mol. Biol.* **293**, 1195–1210
- Mello, C. C., and Barrick, D. (2003) *Protein Sci.* **12**, 1522–1529
- Lin, T. Y., and Timasheff, S. N. (1994) *Biochemistry* **33**, 12695–12701
- Yancey, P. H., and Somero, G. N. (1979) *Biochem. J.* **183**, 317–323
- Bagnasco, S. M., Balaban, R. Fales, H. M., Yang, Y. M., and Burg, M. B. (1986) *J. Biol. Chem.* **261**, 5872–5877
- Garcia-Perez, A., and Burg, M. B. (1990) *Hypertension* **16**, 595–602
- Nakanishi, T., Uyama, O., Nakahama, H., Takamitsu, Y., and Sugita, M. (1993) *Am. J. Physiol.* **264**, F472–F479
- Yancey, P. H. (1985) in *Transport Processes, Iono- and Osmoregulation* (Gilles, R., and Gilles-Ballien, M., eds) pp. 424–436, Springer-Verlag, Berlin, Germany
- Yancey, P. H., and Somero, G. N. (1980) *J. Exp. Zool.* **212**, 205–213
- Boyd, T. A., Cha, C. J., Forster, R. P., and Goldstein, L. (1977) *J. Exp. Zool.* **199**, 435–442
- Forster, R. P., and Goldstein, L. (1976) *Am. J. Physiol.* **230**, 925–931
- Wang, A., and Bolen, D. W. (1996) *Biophys. J.* **71**, 2117–2122
- Sadqi, M., Lapidus, L. J., and Munoz, V. (2003) *Proc. Natl. Acad. Sci. U. S. A.* **100**, 12117–12122
- Garcia-Mira, M. M., Boehringer, D., and Schmid, F. X. (2004) *J. Mol. Biol.* **339**, 555–569
- Sali, A., Shakhnovich, E., and Karplus, M. (1994) *Nature* **369**, 248–251
- Gutin, A. M., Abkevich, V. I., and Shakhnovich, E. I. (1995) *Biochemistry* **34**, 3066–3076
- Noppert, A., Gast, K., Zirwer, D., and Damaschun, G. (1998) *Fold. Des.* **3**, 213–221
- Rami, B. R., and Udgaonkar, J. B. (2002) *Biochemistry* **41**, 1710–1716
- Rami, B. R., Krishnamoorthy, G., and Udgaonkar, J. B. (2003) *Biochemistry* **42**, 7986–8000
- de Gennes, P. G. (1985) *J. Phys. Lett.* **46**, L639–L642

Osmolytes Induce Structure in an Early Intermediate on the Folding Pathway of Barstar

Lovy Pradeep and Jayant B. Udgaonkar

J. Biol. Chem. 2004, 279:40303-40313.

doi: 10.1074/jbc.M406323200 originally published online July 17, 2004

Access the most updated version of this article at doi: [10.1074/jbc.M406323200](https://doi.org/10.1074/jbc.M406323200)

Alerts:

- [When this article is cited](#)
- [When a correction for this article is posted](#)

[Click here](#) to choose from all of JBC's e-mail alerts

This article cites 58 references, 8 of which can be accessed free at <http://www.jbc.org/content/279/39/40303.full.html#ref-list-1>